The International Journal of Advanced Manufacturing Technology
https://doi.org/10.1007/s00170-024-12965-6

ORIGINAL ARTICLE

Solving basic problems of compliant tolerance analysis by static analogy

Antonio Armillotta[1]

Received: 5 May 2023 / Accepted: 2 January 2024

Abstract
Predicting the geometric variation of sheet metal assemblies is a complex task, because deformation during joining operations influences the propagation of initial part deviations. To consider this effect, the paper proposes a method that formulates tolerance analysis as an equivalent problem of static analysis. Previously proposed for rigid parts, the static analogy is extended to compliant parts and applied to two-dimensional problems modeled with straight beams under the assumptions of small displacements and normal distributions of errors. For such simple cases, the method solves the problem by linearization, avoiding the use of Monte Carlo simulation and the related computational burden. Compared to existing linearization methods, the static analogy is less efficient in the integration with a finite element solver. However, it features an especially simple procedure that does not require the calculation of deflections, thus allowing a streamlined solution and even manual calculations. The comparison with alternative methods provides a first verification of the feasibility of the method, in view of further developments with the aim of dealing with cases of realistic complexity.

Keywords Tolerancing · Variation simulation · Sheet metal assembly · Fixturing · Spot welding

1 Introduction

Tolerance analysis evaluates the impact of part manufacturing errors on the variation of assembly-level functional requirements, i.e., geometric conditions involving different parts. The task has been traditionally carried out on machined parts, which are thick and rigid in order to effectively transmit forces and motions in mechanisms. In such cases, calculating the propagation of errors between mating parts is a purely geometric problem, which can be solved with several models of rigid body transformations [1, 2]. However, the rigid body assumption does not apply to sheet metal parts, widely used for car bodies and aircraft structures. These deform during assembly operations (e.g. spot welding or riveting) creating additional sources of variation.

The combined effect of manufacturing and assembly errors can be evaluated by solving a more complex problem, often referred to as compliant tolerance analysis. In their nominal geometry, the parts would fit together perfectly and their joining would cause no deformation. Geometric errors from sheet metalworking processes create gaps between the parts, which must be clamped by assembly tools to restore their effective contact. After joining and releasing, the assembly springs back and deviates from its nominal shape. The amount of distortion could be calculated by well-known procedures for the static analysis of overconstrained frames. In practice, calculations are carried out using the finite element method (FEM), which applies a common procedure to any configuration specified in input. In a Monte Carlo simulation, the FEM analysis must be repeated many times with randomly generated errors consistent with part tolerances. This can involve long computation times, as well as difficulties in evaluating the contributions of individual tolerances to the assembly variation.

Several methods have been proposed in literature to reduce the number of needed FEM runs. They are mostly based on linear models of springback as a function of part errors at selected points. The linearization has the advantage of avoiding Monte Carlo simulation and allowing the explicit calculation of the sensitivities of assembly errors to individual part errors [3].

The paper proposes a new linearization method for compliant tolerance analysis. It is based on a static analogy,

✉ Antonio Armillotta
antonio.armillotta@polimi.it

[1] Dipartimento Di Meccanica, Politecnico Di Milano, Via La Masa 1, 20156 Milan, Italy

Published online: 16 January 2024

which reduces the problem to the calculation of internal forces on the parts when the assembly is loaded with appropriate external forces. Like existing methods, the static analogy avoids Monte Carlo simulation and requires a limited number of FEM runs. As a potential advantage, the method does not need to calculate displacements from internal forces. This simplifies the steps of the procedure, to the extent that particularly simple cases could be solved by hand calculations or using known results of statics.

In the following, the static analogy will be described and compared with existing methods on an elementary case that can be treated with a two-dimensional beam model. In literature, the same case has been often used for demonstration purposes and can highlight the potential and limitations of the static analogy. It should be noted, however, that existing methods are not limited to simple 2D cases but have been implemented in commercial software tools to treat realistic 3D cases. For this reason, the comparison will only concern the workflow and computational issues, while the level of complexity of the problems that can be treated is currently limited for the proposed method.

The remainder of the paper is structured as follows. Section 2 reviews existing methods for compliant tolerance analysis. Section 3 illustrates the demonstrative case and the underlying assumptions. Section 4 describes the method based on static analogy, recalls two methods for its validation, and details the procedure for the random generation of part errors from tolerances. Section 5 presents the results and validation of the method. Section 6 discusses the potential of the static analogy in comparison with existing methods. Section 7 summarizes the results and outlines further developments required.

2 Related work

Tolerance analysis verifies that a given set of part tolerances satisfies predefined functional requirements for the assembly. From this perspective, it is not clear whether the flexibility of sheet metal parts requires tighter or looser tolerances to meet a given assembly specification. On the one hand, it leads to additional errors in the assembly process. On the other hand, it lets the parts comply with assembly tools and partially compensate their initial deviations from nominal geometry [4]. Methods for compliant tolerance analysis have been introduced to capture the balance of these two effects.

A first category of methods is based on the direct Monte Carlo (DMC) approach. A first FEM model of the parts before joining is used to calculate the clamping forces from randomly generated errors consistent with part tolerances. The springback is then calculated from the same forces using a second FEM model of the joined parts. The springback variation (i.e., means and standard deviations of displacements at selected points) is finally estimated by repeating the two FEM analyses for a sample of random instances of input errors. The first studies have dealt with 2D cases under the assumptions of linear elastic deformation and simultaneous joining operations. The proposed FEM models are based on either beam elements [5, 6] or offset beam elements to ensure the congruence of the deformations of mating parts [4, 7, 8]. Solid models have also been used for 3D cases with flat parts [9]. For more complex cases, the DMC seems to be a less practical approach due to computational difficulties; these include the large number of FEM runs required for Monte Carlo simulation and need to interface the procedure with a commercial FEM solver.

A significant reduction of the computational effort was achieved with the method of influence coefficients (MIC) [3]. In a first step, the method calculates the influence coefficients, i.e., the displacements at the joints (e.g., spot welds) caused by unit forces at each of the points of interest for the variation; the clamping forces are calculated by inverting the matrix of influence coefficients. In a second step, the assembly is loaded with the clamping forces to calculate the displacements at the variation points; these provide the sensitivities of the same displacements to part errors. Each of the two steps requires just one FEM run for each variation point. Statistical tolerance analysis can be done using the sensitivities without the need of wrapping the procedure in a Monte Carlo simulation.

The MIC has been later extended to account for initially neglected effects. In [10], the accumulation of errors across assembly line stations is treated by integrating the method into a state-space model deriving from the stream-of-variation theory [11, 12]. In [13], the principal component analysis (PCA) on measured data is used to model the dependence between the errors in nearby points due to surface continuity (geometric covariance), reducing it to a vector of independent deviations (variation patterns) for the calculation of the clamping forces in the first step of the MIC. For the same purpose, [14, 15] propose the designated component analysis (DCA) to identify the variation patterns a priori, and then statistically test them on the data. More complex models of geometric covariance are obtained by combining the MIC with various statistical shape models [16–18]. By neglecting less relevant patterns, the MIC-covariance methods further reduce the number of needed FEM runs; their accuracy has been verified experimentally with good results in [19]. Other studies have modified the MIC to avoid that the calculated deformation leads to penetration between the parts; different algorithms for contact modeling are proposed in [20–23]. In [24, 25], the MIC is completed with the calculation of the stresses induced by clamping forces.

Modified versions of the MIC have been proposed to improve the efficiency or detail of the analysis. To simplify the procedure, the influence matrix method of [26, 27]

computes the clamping forces applying unit displacements in the first step of the MIC; the approach is combined with a linear contact algorithm in [28–30]. A further reduction of the number of FEM runs in the first step is achieved with the super-element method of [31–33], which includes a procedure for an efficient evaluation of FEM stiffness matrices. This last feature is also useful for treating cases with both rigid and flexible parts, as previously proposed in [34]; with the same goal, [35] combines the MIC with a method based on 2D transformation matrices to separately treat out-of-plane sheet metal deformation and in-plane rigid body displacements. Other variants of the MIC include a separate calculation of sensitivities to different sources of variation [36, 37], and an additional FEM step with a finer mesh to generate detailed error maps [38].

The efficiency of the MIC comes at the price of some uncertainty due to the linear approximation and to the use of FEM models with static stiffness matrices under the assumption of small displacements. Although such compromise is considered acceptable in practical applications, some studies have proposed more complex methods to exploit the capabilities of advanced FEM tools, while accepting the computational burden of Monte Carlo simulation. Nonlinear FEM has been used to test more accurate contact models based on steady-state contact mechanics [39–42], friction forces [43], quadratic programming [44], sensitivity-free probability analysis [45–47], Timoshenko beam theory [48], and Mindlin plate theory [49, 50]. Other methods combine FEM with models based on transformation vectors or matrices to deal with both rigid and flexible parts [51–54], with statistical shape models to deal with form errors [55], or with multi-objective optimization algorithms for assemblies loaded with external forces [56]. Meshing is another possibly critical aspect in FEM-based methods; to avoid it, a method based on iso-geometric analysis [57, 58] adds errors to NURBS curves and surfaces by means of displacements of their control polygons.

The above methods cover a range of joining processes and do not generally take detailed process features into account. Many studies have tried to tailor DMC and MIC approaches to specific processes. Citing only a few representative references, the main aspects covered include the evolution of deformation along the sequence of operations in spot welding [59] and riveting [60], thermal effects in seam welding processes [61–63], anisotropy, and differential shrinkage of composite parts [64, 65]. Applications of compliant tolerance analysis have also been proposed for related problems, such as fault diagnosis [66–69], fixture layout design [70, 71], tolerance allocation [72–74], statistical process control [75], and the optimization of the spot welding sequence [76–78]. For these purposes, several commercial software packages are now available with increasing functionalities [79]; they are proposed as tools for developing digital twins of sheet metal products and related assembly processes [80].

A common aspect among the methods for compliant tolerance analysis is the pursue of completely different approaches from those applying to rigid parts. Differently, the static analogy proposed in this paper is an attempt to extend a method initially proposed for the tolerance analysis of rigid assemblies, structures, and mechanisms [81–83]. This seems reasonable because the idea of converting tolerance analysis into an equivalent force analysis problem stems from the virtual work principle, which has general validity albeit with possible differences in applications. Since the solution of the problem requires static calculations, the method lends itself naturally to the use of FEM tools. However, these are not required to compute displacements due to clamping forces or vice versa, but only serve to compute internal forces on overconstrained assemblies, where free body diagrams cannot be easily solved. The hypothesis that will be tested below is that this feature leads to a simpler procedure, which may in principle be compatible with alternative ways of calculating forces.

3 Problem and assumptions

The simplest case in compliant tolerance analysis is the spot welding of flat sheet metal. Two rectangular parts are placed on welding fixtures and connected with multiple spot welds in a horizontal lap joint (Fig. 1a). This work will deal with a 2D version of the same case: a single spot weld is made on the two parts, represented in a sectional plane including the

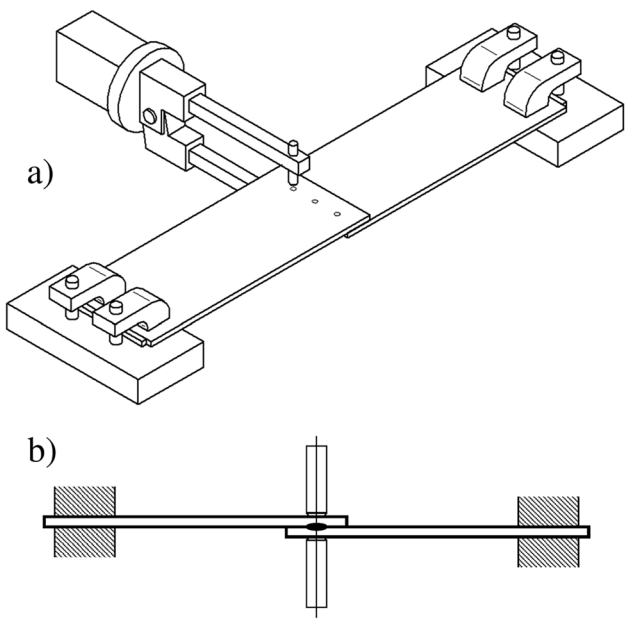

Fig. 1 Joining operation: **a** actual 3D layout; **b** 2D case

welding tool and the two fixtures (Fig. 1b). The parts deform elastically during the operation due to their initial geometric errors; it is assumed that the deformation is uniform along the width of the parts, and does not include the effect of thermal stresses arising in the welding process. For this reason, the case is also representative of different joining processes (e.g., adhesive bonding and fastening with bolts or rivets) where the parts are clamped together to ensure contact.

The joining operation is a sequence of actions that will be referred to as the place-clamp-weld-release (PCWR) cycle. Due to inevitable geometric errors, the parts are not perfectly flat and do not come into actual contact after fixturing (Fig. 2a). The welding tool clamps the parts together forcing them into contact; soon after, it creates the spot weld in the nominal position (Fig. 2b). Finally, the welding tool is released, and the elastic stresses induced in the parts during clamping cause springback of the weldment (here referred to as the "assembly"): the joint moves vertically with respect to the nominal plane, and the assembly distorts to accommodate the displacement of the joint (Fig. 2c).

The tolerance analysis problem consists in evaluating the distortion in the assembly from the initial geometric errors in the two parts. If the errors are given, the distortion will be calculated deterministically. More commonly, the errors are assumed to vary randomly within limits allowed by tolerances; in this case, the distortion will be estimated statistically. In particular, tolerance limits will be regarded as $\pm 3\sigma$ limits of normal distributions; the same assumption will be made on the variation of distortion.

In more detail, the geometric errors are defined as the profile deviations in the parts once they are placed in their fixtures. In an XY coordinate system with origin at the joint location, the unsupported end of each part should be in a nominal vertical position ($y=0$) and in a nominal angular position ($y'=\mathrm{d}y/\mathrm{d}x=0$). The errors on the left (1) and right (2) parts are thus expressed as linear displacements δ_i and angular displacements θ_i (equal to y' derivatives due to the assumption of small displacements) at the joint location, with $i=1, 2$. In Fig. 3a, all the errors are shown with a positive sign (upward and counterclockwise), and only the length of each part between the fixture and the joint is considered.

After welding, the distortion at the joint location includes a linear displacement δ and an angular displacement θ. At the same time, the whole assembly deflects; the analysis will provide the linear displacements y_j on a set of points $j=1, 2, \ldots n$ sampled along X on the assembly (Fig. 3b).

The data for the analysis include the thicknesses t_i and the lengths l_i of the two parts, as well as their common width w and the elastic moduli E_i of the respective materials. The second moment of area of each part is calculated as $I_i=b_i t_i^2/12$.

In addition to manufacturing errors in the parts, tooling errors may have an influence on distortion. In particular, the two fixtures and the welding tool can have linear and angular deviations from their nominal positions. Although these further errors are neglected in the calculations below, their treatment will be explained in the description of the proposed method.

4 Methods

The solution of the problem described in Section 3 consists in building a linear model of the output errors on the assembly as a function of the input errors on the parts:

$$\begin{bmatrix} y_1 \\ y_2 \\ \cdots \\ y_n \end{bmatrix} = \begin{bmatrix} s_{11} & s_{12} & s_{13} & s_{14} \\ s_{21} & s_{22} & s_{23} & s_{24} \\ \cdots & \cdots & \cdots & \cdots \\ s_{n1} & s_{n2} & s_{n3} & s_{n4} \end{bmatrix} \begin{bmatrix} \delta_1 \\ \theta_1 \\ \delta_2 \\ \theta_2 \end{bmatrix} \tag{1}$$

where s_{j1}, s_{j2}, s_{j3}, and s_{j4} are the sensitivities of the vertical displacement y_j ($j=1, 2, \ldots n$) to the four errors δ_1, θ_1, δ_2, and θ_2. Such linearization is not strictly necessary: for

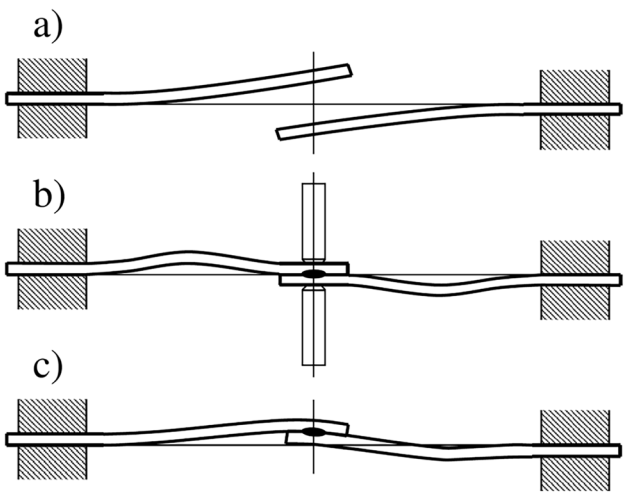

Fig. 2 PCWR cycle: **a** place; **b** clamp and weld; **c** release

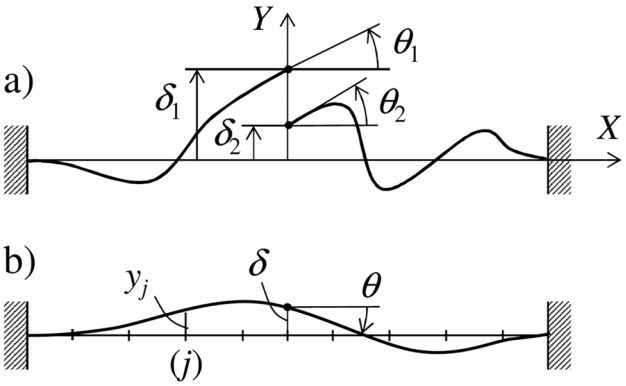

Fig. 3 Geometric errors: **a** on the parts; **b** on the assembly

example, Monte Carlo simulation could estimate the output error distributions from the input error distributions through any, possibly nonlinear, model of error propagation. However, obtaining sensitivities is useful for a quick assessment of the contributions of individual tolerances to assembly variation, which greatly helps the related design task of tolerance allocation.

4.1 Static analogy

The method based on the static analogy was previously proposed for rigid tolerance analysis [81–83]. Here, the method will be demonstrated on the compliant parts involved in the PCWR case. The extension is reasonable because it satisfies the main premise of the static analogy, illustrated in Fig. 4. Let F be an external force applied to an assembly constrained by a support. If a part i is removed from the assembly, the equilibrium can be maintained by loading the adjacent parts with a force opposite to the internal force F_i. According to the principle of virtual work, the sum of the virtual works done by the external forces F and $-F_i$ for a pair of compatible virtual displacements is equal to zero. Let δ_i be a geometric error on part i in the direction of F_i and δ the consequent geometric error on the assembly in the direction of F. Considering the errors as virtual displacements and assuming bilateral constraints between parts, the equilibrium condition is

$$F\delta - F_i\delta_i = 0 \tag{2}$$

This gives the relationship between δ and δ_i:

$$\delta = \frac{F_i}{F}\delta_i \tag{3}$$

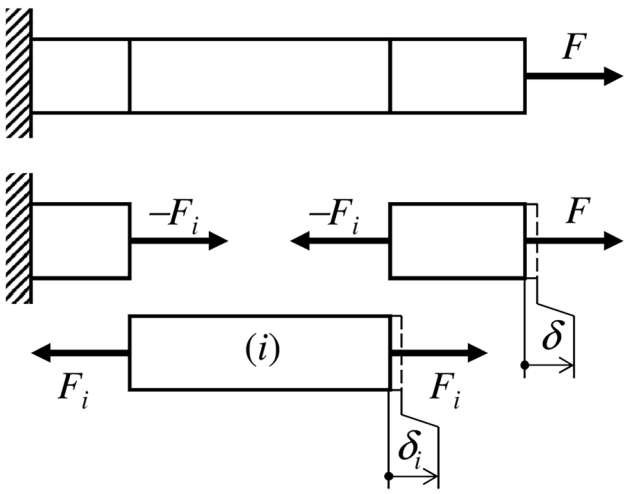

Fig. 4 Tolerance analysis by static analogy

The ratio F_i/F is thus the sensitivity of the assembly error δ to an error δ_i on part i. This means that a tolerance analysis problem can be solved with an equivalent static model, where the assembly error corresponds to an external force and the part errors correspond to internal forces. The calculation of sensitivities comes down to the resolution of the static model, which gives the internal forces corresponding to all part errors. Equation (3) can be generalized to angular errors, which correspond to torques. The same static model can be used to calculate the sensitivity of the assembly error to a position error of a support; in this case the force F_i in (3) is opposite to the support reaction, so as to have the same direction as the virtual displacement δ_i corresponding to the error in the support.

The static analogy can be applied to the PCWR case in two steps. In the first one, the distortion of the assembly at the joint location is calculated as a function of the errors in the parts:

$$\begin{bmatrix}\delta\\ \theta\end{bmatrix} = \begin{bmatrix}s_{\delta 1} & s_{\delta 2} & s_{\delta 3} & s_{\delta 4}\\ s_{\theta 1} & s_{\theta 2} & s_{\theta 3} & s_{\theta 4}\end{bmatrix}\begin{bmatrix}\delta_1\\ \theta_1\\ \delta_2\\ \theta_2\end{bmatrix} \tag{4}$$

In the second, the displacements at points along the assembly are calculated as a function of the distortion at the joint location:

$$\begin{bmatrix}y_1\\ y_2\\ \cdots\\ y_n\end{bmatrix} = \begin{bmatrix}s_{1\delta} & s_{1\theta}\\ s_{2\delta} & s_{2\theta}\\ \cdots & \cdots\\ s_{n\delta} & s_{n\theta}\end{bmatrix}\begin{bmatrix}\delta\\ \theta\end{bmatrix} \tag{5}$$

Therefore, the sensitivity matrix in (1) is the product of two sensitivity matrices calculated in the two steps:

$$\begin{bmatrix}s_{11} & s_{12} & s_{13} & s_{14}\\ s_{21} & s_{22} & s_{23} & s_{24}\\ \cdots & \cdots & \cdots & \cdots\\ s_{n1} & s_{n2} & s_{n3} & s_{n4}\end{bmatrix} = \begin{bmatrix}s_{1\delta} & s_{1\theta}\\ s_{2\delta} & s_{2\theta}\\ \cdots & \cdots\\ s_{n\delta} & s_{n\theta}\end{bmatrix}\begin{bmatrix}s_{\delta 1} & s_{\delta 2} & s_{\delta 3} & s_{\delta 4}\\ s_{\theta 1} & s_{\theta 2} & s_{\theta 3} & s_{\theta 4}\end{bmatrix} \tag{6}$$

The first step requires two equivalent static models; both include a horizontal beam (the assembly) fixed at both ends (the welding fixtures). The first model applies an upward unit force (corresponding to δ) to the beam at the joint location (Fig. 5a). The separation of the two parts at the joint gives two exactly constrained free-body diagrams, which are solved by applying equilibrium equations. The internal forces and torques at the free ends of the two parts give the sensitivities $s_{\delta i}$ in (4). The second model applies a unit torque (corresponding to θ) to the assembly at the joint location (Fig. 5b). On the two free-body diagrams, the internal forces and torques provide the sensitivities $s_{\theta i}$ in (4).

In the second step, an upward unit force (corresponding to y_j) is applied to point j of a beam corresponding to the

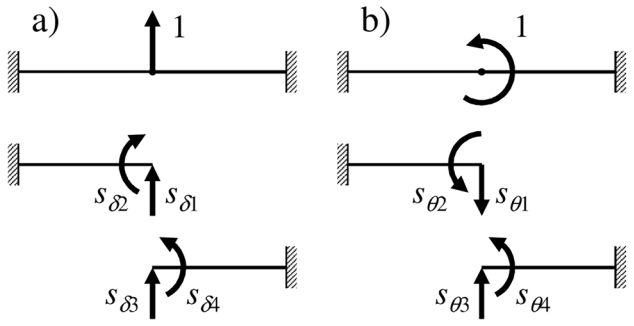

Fig. 5 Equivalent static models for the distortion at the joint: **a** δ; **b** θ

part the point belongs to. The beam is fixed at both ends: one of the supports is a welding fixture, while the other corresponds to the nominal condition $\delta = \theta = 0$. Solving the over-constrained beam gives a reaction force and a reaction torque at the joint-side support. The opposite force and torque correspond respectively to displacements δ and θ of the support; consequently, they provide the sensitivities $s_{j\delta}$ and $s_{j\theta}$ in (5). Figure 6a and b illustrate the details of the equivalent static model in cases where point j is on part 1 or 2, respectively.

4.2 Validation

The correctness of the static analogy will be verified using two existing methods: the direct method and the method of influence coefficients. The comparison will also allow to discuss possible advantages and limitations of the proposed method regarding computational efficiency and application to more complex cases.

The direct method [7] consists in calculating the elastic reactions during clamping for a given set of errors in the parts, and applying them to the assembly to calculate the distortion. When coupled with the random generation of input errors, it is referred to as the direct Monte Carlo (DMC) method. In the PCWR case, the two steps must be repeated for the four errors δ_1, θ_1, δ_2, and θ_2. For each error,

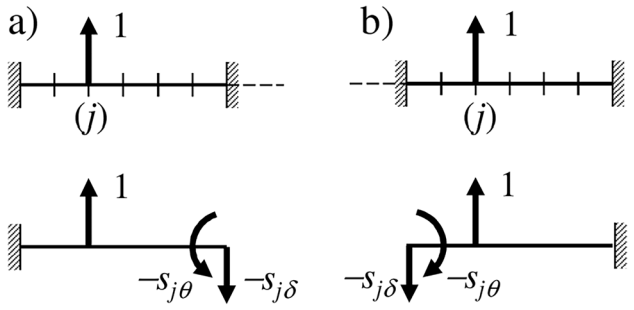

Fig. 6 Equivalent static model for the distortion at point j: **a** on part 1; **b** on part 2

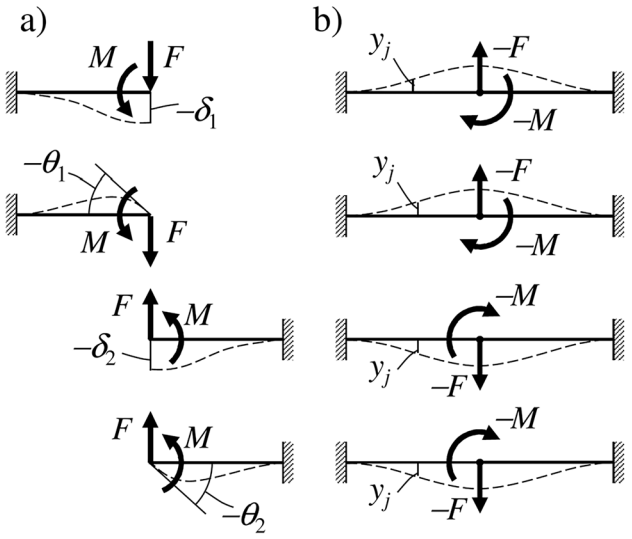

Fig. 7 DMC method: **a** clamping reactions; **b** distortions along the assembly

a linear or angular displacement in the opposite direction is applied to the corresponding part (1 or 2) modeled as a cantilever beam; the resolution of the beam provides the force F and the torque M that must be applied to the part to cancel the error during clamping (Fig. 7a). The force $-F$ and the torque $-M$ are then applied to the assembly modeled as a beam fixed at both ends; its resolution gives the errors y_j at all points of interest (Fig. 7b).

The method of influence coefficients (MIC, [3]) will be used only to calculate the sensitivities in (4). For this purpose, unit forces and torques are first applied to parts 1 and 2 modeled as cantilever beams (Fig. 8a). Each of the four load cases provides linear and angular displacements at the unsupported end of the beam, which form the matrix of influence coefficients:

$$\mathbf{C} = \begin{bmatrix} c_{11} & c_{12} & 0 & 0 \\ c_{21} & c_{22} & 0 & 0 \\ 0 & 0 & c_{33} & c_{34} \\ 0 & 0 & c_{43} & c_{44} \end{bmatrix} \tag{7}$$

where the c_{ij} coefficient corresponds to the ith load case and to the jth part error. The stiffness matrix

$$\mathbf{K} = \mathbf{C}^{-1} = \begin{bmatrix} k_{11} & k_{12} & 0 & 0 \\ k_{21} & k_{22} & 0 & 0 \\ 0 & 0 & k_{33} & k_{34} \\ 0 & 0 & k_{43} & k_{44} \end{bmatrix} \tag{8}$$

it is then multiplied by a matrix of unit part errors

$$\mathbf{V} = \begin{bmatrix} 1 & 0 \\ 0 & 1 \\ 1 & 0 \\ 0 & 1 \end{bmatrix} \tag{9}$$

to get the matrix of clamping forces:

$$\mathbf{F_C} = \mathbf{KV} = \begin{bmatrix} f_{11} & f_{12} \\ f_{21} & f_{22} \\ f_{31} & f_{32} \\ f_{41} & f_{42} \end{bmatrix} \tag{10}$$

where f_{i1} and f_{i2} are the clamping force and torque corresponding to the ith unit part error, with $i = 1, 2, 3, 4$ for δ_1, θ_1, δ_2, and θ_2, respectively. Finally, the clamping forces are applied to the assembly modeled as a beam fixed at both ends (Fig. 8b); the linear and angular displacements calculated at the joint location give the sensitivity matrix in (4).

In all the above methods (static analogy, DMC, MIC), some structures have to be solved to calculate the required forces or displacements. In the simplest cases (individual parts, or symmetrical assemblies), the calculations will be done analytically or using known results of statics. In generic cases or when the random generation of part errors is required, the calculations will be carried out with the finite element method (FEM): the structures will be modeled through horizontal beam elements with the following stiffness matrix:

$$\mathbf{k} = \frac{EI}{l^2} \begin{bmatrix} 12 & 6l & -12 & 6l \\ 6l & 4l^2 & -6l & 2l^2 \\ -12 & -6l & 12 & -6l \\ 6l & 2l^2 & -6l & 4l^2 \end{bmatrix} \tag{11}$$

where l is the length of the beam element (which can be the whole length of the part or a fraction thereof), while E and I are evaluated for the part the element belongs to. The rows of $\mathbf{k}$ are associated with the forces and torques in the two nodes of the element, while the columns are associated with the respective linear and angular displacements.

4.3 Simulation

Once validated, the static analogy will be used to analyze the contribution of part tolerances to distortion. For this purpose, tolerances could be specified separately on part errors δ_1, θ_1, δ_2, and θ_2. Each tolerance would be treated as the $\pm 3\sigma$ limit of a normal distribution with zero mean, with the aim of estimating the corresponding limit on the displacements y_j ($j = 1, 2, \ldots n$) at the points along the assembly.

Such a choice, however, would not account for possible statistical correlations between the error variables. If it were assumed that the two parts are subject to a random form error without further specification, the δ_i and θ_i on the same part would be statistically independent. Differently, it is often assumed that the two parts bend and are clamped by the welding tool with a vertical force, considered sufficient to bring them back to the correct position and orientation. This is

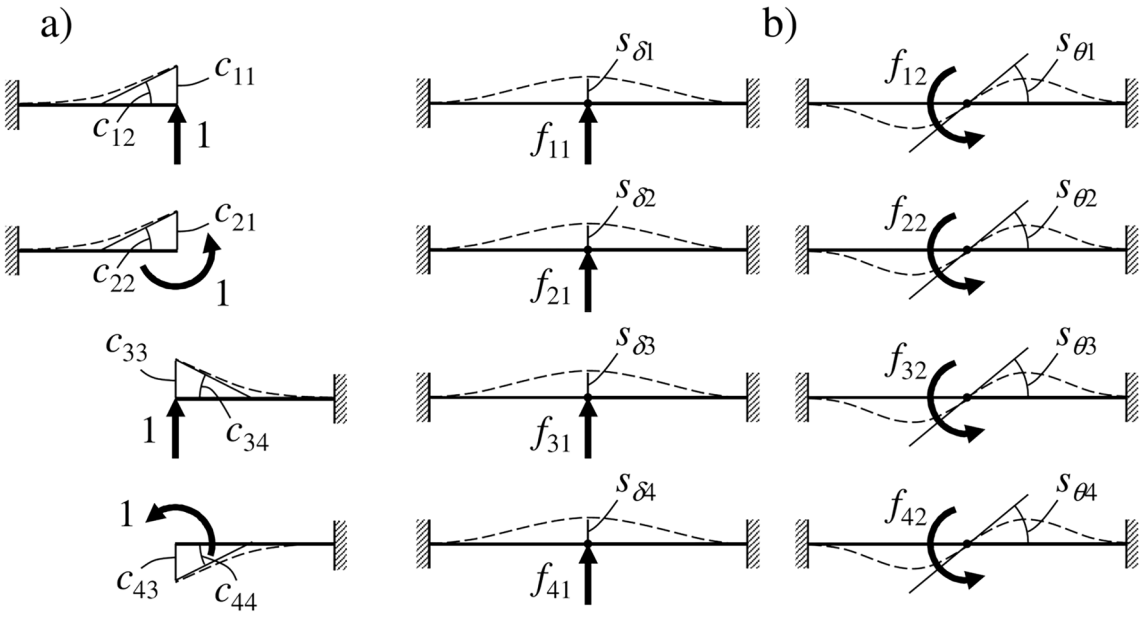

Fig. 8 MIC method: **a** influence coefficients; **b** sensitivities

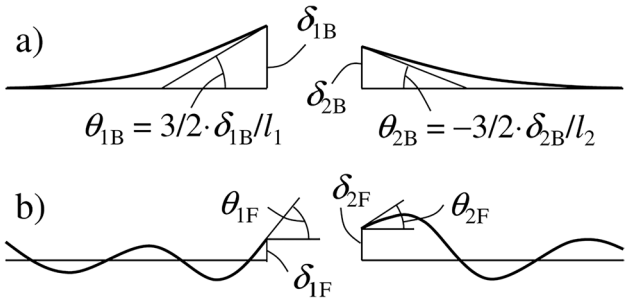

Fig. 9 Components of part errors: **a** bending; **b** form error

equivalent to assuming that the input error in each part is equal to the deflection caused by a vertical end force on a cantilever beam. If this is true, δ_i and θ_i on the same part are not statistically independent, as they are related by the following equation:

$$\theta_i = \pm\frac{3}{2}\frac{\delta_i}{l_i} \tag{12}$$

with plus or minus sign respectively for parts 1 and 2. To cover both cases, it will be assumed that each part is subject to two error components. The first is a bending deflection, limited by tolerances $\pm T_{B1}$ and $\pm T_{B2}$. The second is a random form error, limited by straightness tolerances T_{F1} and T_{F2} (or by flatness tolerances in the 3D case).

Figure 9 illustrates how part errors are randomly generated from the specified tolerances. On each part, the linear and angular errors include the two components of deflection and form error:

$$\delta_i = \delta_{iB} + \delta_{iF} \tag{13}$$

$$\theta_i = \theta_{iB} + \theta_{iF} \tag{14}$$

with $i = 1, 2$. While the θ_{iB} are calculated as in (12), the other three components are normally distributed with zero mean and standard deviations depending on the tolerances as detailed in Table 1. The standard deviation on θ_{iF} is a first approximation based on a simplifying assumption: the form profile on each part is a sine wave with wavelength λ_F:

$$y_i = \frac{T_{Fi}}{2}\sin\frac{2\pi x_i}{\lambda_F} \tag{15}$$

where y_i is the vertical deviation of the form profile and x_i is the horizontal coordinate referred to a given origin on the part. Consequently, the angular error along the form profile is

$$\theta_{iF} \approx y_i' = \frac{\pi T_{Fi}}{\lambda_F}\cos\frac{2\pi x_i}{\lambda_F} \tag{16}$$

and varies between the two limits $\pm\pi T_{Fi} / \lambda_F$. The standard deviation on θ_{iF} is obtained by interpreting T_{Fi} as twice the 3σ limit on the linear error, and approximating the actual angular error distribution with a normal. This provides a rough estimate of the variation on the angular error, which could be improved by using more complex statistical shape models.

The tolerance analysis is based on the results of the static analogy for the distortion y_j at each point of the assembly ($j = 1, 2, \ldots n$):

$$y_j = s_{j1}\delta_1 + s_{j2}\theta_1 + s_{j3}\delta_2 + s_{j4}\theta_2 \tag{17}$$

where the sensitivities are defined as in (6). Considering the dependence between δ_{iB} and θ_{iB} in (12), the output variance includes two covariance terms:

$$\begin{aligned}\mathrm{var}y_j = {} & s_{j1}^2\mathrm{var}\delta_1 + s_{j2}^2\mathrm{var}\theta_1 + s_{j3}^2\mathrm{var}\delta_2 + s_{j4}^2\mathrm{var}\theta_2 \\ & +2s_{j1}s_{j2}\mathrm{cov}\left(\delta_1,\theta_1\right) + 2s_{j3}s_{j4}\mathrm{cov}\left(\delta_2,\theta_2\right)\end{aligned} \tag{18}$$

Then, the errors are split into the two components as in (13) and (14), and the standard deviations in Table 1 are introduced in Eq. (18). Furthermore, it is easily verified that

$$\mathrm{cov}\left(\delta_i,\theta_i\right) = \pm\frac{3}{2l_i}\sigma_{iB}^2 \tag{19}$$

The resulting output variance is

$$\begin{aligned}\mathrm{var}y_j = {} & \left(s_{j1}^2 + \frac{9}{4l_1^2}s_{j2}^2 + \frac{3}{l_1}s_{j1}s_{j2}\right)\sigma_{1B}^2 + \left(s_{j1}^2 + \frac{4\pi^2}{\lambda_F^2}s_{j2}^2\right)\sigma_{1F}^2 \\ & +\left(s_{j3}^2 + \frac{9}{4l_2^2}s_{j4}^2 - \frac{3}{l_2}s_{j3}s_{j4}\right)\sigma_{2B}^2 + \left(s_{j3}^2 + \frac{4\pi^2}{\lambda_F^2}s_{j4}^2\right)\sigma_{2F}^2\end{aligned} \tag{20}$$

and corresponds to the following root-sum-square (RSS) tolerance stackup at the jth point:

$$T_j^2 = s_{jB1}^2T_{B1}^2 + s_{jF1}^2T_{F1}^2 + s_{jB2}^2T_{B2}^2 + s_{jF2}^2T_{F2}^2 \tag{21}$$

where the sensitivities of the specified tolerances are

$$s_{jB1} = \sqrt{s_{j1}^2 + \frac{9}{4l_1^2}s_{j2}^2 + \frac{3}{l_1}s_{j1}s_{j2}} \tag{22}$$

$$s_{jF1} = \frac{1}{2}\sqrt{s_{j1}^2 + \frac{4\pi^2}{\lambda_F^2}s_{j2}^2} \tag{23}$$

$$s_{jB2} = \sqrt{s_{j3}^2 + \frac{9}{4l_2^2}s_{j4}^2 - \frac{3}{l_2}s_{j3}s_{j4}} \tag{24}$$

$$s_{j\mathrm{F}2} = \frac{1}{2}\sqrt{s_{j3}^2 + \frac{4\pi^2}{\lambda_{\mathrm{F}}^2}s_{j4}^2} \tag{25}$$

5 Results

The following subsections describe the validation of the method based on the static analogy on examples of increasing complexity, and its use to estimate the stackup of tolerances.

5.1 Analytic solution

A first validation example is a symmetrical PCWR case, where the parts have the same material (E), length (l), and section (w, t, I). Static calculations are simple enough to allow an analytical comparison with the other methods. For simplicity, the problem is limited to calculating the distortion at the joint location (δ and θ).

For the static analogy, the equivalent static models are overconstrained yet easily solved from known results of statics (Fig. 10). Considering the correspondence between internal forces and part distortions, the following sensitivity matrix results:

$$\begin{bmatrix} s_{\delta 1} & s_{\delta 2} & s_{\delta 3} & s_{\delta 4} \\ s_{\theta 1} & s_{\theta 2} & s_{\theta 3} & s_{\theta 4} \end{bmatrix} = \begin{bmatrix} 1/2 & -l/4 & 1/2 & l/4 \\ -3/4l & 1/2 & 3/4l & 1/2 \end{bmatrix} \tag{26}$$

The method could also allow an easy estimate of the influence of linear and angular errors in the welding fixtures (elsewhere neglected in this paper). The sensitivities of δ and θ with respect to these errors is opposite to the reaction forces and torques at the two supports, respectively, under the unit external force (Fig. 10a) and the unit external torque (Fig. 10b). For example, if $l = 300$ mm, a 1-mm upward displacement of the left support would have the effect of increasing δ by 0.5 mm and decreasing θ by $3/(4l) = 0.0025$ rad $= 0.14°$.

For the analytical solution with the direct method (Fig. 7), it is first noted that a force F applied to the end of a cantilever beam (a part before welding) causes the following deflection and rotation:

$$\delta_F = \frac{Fl^3}{3EI},\ \theta_F = \pm\frac{Fl^2}{2EI} \tag{27}$$

where the $\pm$ signs refer to parts 1 and 2, respectively. Similarly, a torque M causes

$$\delta_M = \pm\frac{Ml^2}{2EI},\ \theta_F = \frac{Ml}{EI} \tag{28}$$

The conditions

$$\begin{cases} \delta_F + \delta_M = \delta \\ \theta_F + \theta_M = \theta \end{cases} \tag{29}$$

lead to the following results for part 1:

$$F_1 = \frac{6EI}{l^3}\left(2\delta_1 - l\theta_1\right),\ M_1 = \frac{2EI}{l^2}\left(-3\delta_1 + 2l\theta_1\right) \tag{30}$$

and for part 2:

$$F_2 = \frac{6EI}{l^3}\left(2\delta_2 + l\theta_2\right), M_2 = \frac{2EI}{l^2}\left(3\delta_2 + 2l\theta_2\right) \tag{31}$$

As the total elastic reactions $(F_1 + F_2)$ and $(M_1 + M_2)$ are applied in the mid-span of the beam fixed at both ends (the assembly), the following deflection and rotation are obtained:

$$\delta = \frac{(F_1+F_2)l^3}{24EI},\ \theta = \frac{(M_1+M_2)l}{8EI} \tag{32}$$

Equations (30), (31), and (32) lead to the following expression of the distortion at joint location:

$$\delta = \frac{\delta_1+\delta_2}{2} - \frac{l}{4}\left(\theta_1 - \theta_2\right),\ \theta = -\frac{3}{4}\frac{\delta_1-\delta_2}{l} + \frac{\theta_1+\theta_2}{2} \tag{33}$$

The sensitivities in (33) are equal to those in (26) calculated with the static analogy.

For the MIC, the static calculations in Fig. 8a result in the following matrix of influence coefficients:

$$\mathbf{C} = \frac{l}{6EI}\begin{bmatrix} 2l^2 & 3l & 0 & 0 \\ 3l & 6 & 0 & 0 \\ 0 & 0 & 2l^2 & -3l \\ 0 & 0 & -3l & 6 \end{bmatrix} \tag{34}$$

Equations (9) and (10) provide the matrix of clamping forces:

$$\begin{aligned} \mathbf{F_C} = \mathbf{KV} = \mathbf{C}^{-1}\mathbf{V} &= \frac{12EI}{l^3}\begin{bmatrix} 1 & -l/2 & 0 & 0 \\ -l/2 & l^3/3 & 0 & 0 \\ 0 & 0 & 1 & l/2 \\ 0 & 0 & l/2 & l^3/3 \end{bmatrix}\begin{bmatrix} 1 & 0 \\ 0 & 1 \\ 1 & 0 \\ 0 & 1 \end{bmatrix} \\ &= \frac{12EI}{l^3}\begin{bmatrix} 1 & -l/2 \\ -l/2 & l^3/3 \\ 1 & l/2 \\ l/2 & l^3/3 \end{bmatrix} \end{aligned} \tag{35}$$

Table 1 Random components of part errors

Error	*Standard deviation*
$\delta_{i\mathrm{B}}$	$\sigma_{i\mathrm{B}} = T_{\mathrm{B}i}/3$
$\delta_{i\mathrm{F}}$	$\sigma_{i\mathrm{F},\delta} = T_{\mathrm{F}i}/6$
$\theta_{i\mathrm{F}}$	$\sigma_{i\mathrm{F},\theta} = \pi T_{\mathrm{F}i}/3\lambda_{\mathrm{F}}$

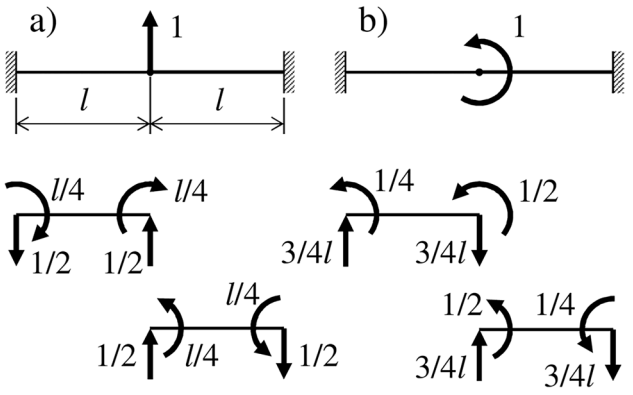

Fig. 10 Symmetric case with static analogy: **a** δ; **b** θ

The forces and torques in $\mathbf{F_C}$ are finally applied to the assembly (Fig. 8b). All the load cases are solved from known results of statics, yielding a sensitivity matrix identical to the one in (26) calculated with the static analogy.

5.2 FEM solution

In general cases, the two sheet metal parts have different lengths and thicknesses, as well as possibly different materials (uncommon in the case of spot welding). Consequently, the static calculations are more complex, because the assembly is overconstrained and not symmetrical. The comparison between the static analogy and the direct method will be done on a numerical example by FEM analysis.

It is assumed that parts 1 and 2 are both made of steel ($E=210$ GPa) and have the same width ($w=500$ mm) but different lengths and thicknesses. The data for the example are listed in Table 2, including the given linear and angular errors at the ends of the two parts. The tolerance analysis will consist in calculating the distortion both at the joint location and at points spaced by $\Delta x=50$ mm between the two fixtures.

For the different steps of the two methods, the FEM models will use elements of appropriate lengths. These include the whole lengths l_1 and l_2 of the parts when forces and deflections are to be calculated at the joint, and length Δx for calculations involving single points along either the parts or the assembly. In the latter case, the two parts are divided into $n_1=6$ and $n_2=4$ elements, and the total number of points is $n=11$.

In the first step of the static analogy (Fig. 5), a unit vertical force and a unit torque at the joint location are separately applied to the assembly, which is modeled with two elements corresponding to the individual parts. In both load cases, the FEM model provides the forces and torques at the joint, which are directly associated with the sensitivities of the joint distortion. Equation (4) becomes

$$\begin{bmatrix}\delta\\ \theta\end{bmatrix}=\begin{bmatrix}0.498 & -0.054 & 0.502 & 0.054\\ -2.702 & 0.679 & 2.702 & 0.321\end{bmatrix}\begin{bmatrix}1\cdot10^{-3}\\ 0.0075\\ -1\cdot10^{-3}\\ 0.009\end{bmatrix}=\begin{bmatrix}0.078\cdot10^{-3}\\ 0.0026\end{bmatrix} \tag{36}$$

with lengths in meters and angles in radians. In the second step, the two parts are modeled with n_1 and n_2 elements, respectively, and are constrained with an additional fixed support at the joint location. The FEM model is subjected to n load cases, where a unit vertical force is applied to one different node (Fig. 6); the analysis of each load case provides the force and reaction torque at the joint support. The opposite force and torque give the sensitivities in the corresponding row of the matrix in (5). Finally, the calculation is completed as in (6) to get the final displacements y_j. Table 3 lists the nodes of the FEM model and their coordinates, sensitivities, and displacements (obviously it is $y_7=\delta$ at the joint).

The above results are verified with the direct method. A first set of four FEM analyses is done on the individual parts modeled with a single element and fixed at the supported end (Fig. 7a). In the ith analysis, a different input error is applied to one of the two parts, and the corresponding clamping forces F_i and torques M_i are calculated. The opposite forces and torques are then applied to the assembly modeled with n_1+n_2 elements (Fig. 7b); a second set of four analyses provides the displacement components y_{ij} associated with each input error. Finally, the distortions y_j are obtained by adding the y_{ij} obtained in the individual analyses. Table 4 shows the results of the two steps of the direct method at the three points with $j=3$ (200 mm to the left of the joint), $j=7$ (joint location), and $j=9$ (100 mm to the right of the joint). A comparison with Table 3 confirms that the total distortion at each point is equal to the one obtained with the static analogy.

The overall distortion of the assembly is shown in Fig. 11. The linear displacements at the n sampled points are exactly the same for the two methods. The asymmetry of the assembly and of the input errors cause an asymmetric output distortion, with both downward and upward profile errors in different sections. The displacement and the rotation are equal to zero at the fixture ends, even if this is not apparent for the rotation due to the low number of elements of the FEM model. For illustration purposes, the thicknesses and the input errors of the two parts are drawn at a different vertical scale (not shown). In particular, the rotations θ_1 and θ_2 are indicated with solid lines at the joint location. Dashed lines are also shown at the same location; these correspond to the rotation at the end of a cantilever beam that gets the same deflection by a vertical end force. If the actual part rotations deviate from

Table 2 Part dimensions and errors for the example

Part	l_i, mm	t_i, mm	δ_i, mm	θ_i, rad
1	300	2	1	0.0075
2	200	1	−1	0.009

pure-bending rotations, the electrodes of the spot welding tool (or the ends of any other type of joining tool) clamp the parts by applying not only a vertical force, but also a torque. This occurs when the two sheet metal parts are brought into contact and the flat ends of the tools force the parts to an horizontal orientation. The clamping torque causes an additional non-symmetrical deflection, which is clearly visible in the distorted profile.

With more closely spaced points ($\Delta x = 10$ mm), Fig. 12 shows the effects of different part errors on the same example. On both parts, the profile deviation at the end comes only from deflection with no random form error, with δ_i and θ_i related by Eq. (12). In Fig. 12a, the linear displacements are equal to those of the previous example ($\delta_1 = 1$ mm, $\delta_2 = -1$ mm): it can be seen that the pure bending leads to a much more symmetrical upward distortion due to the lack of clamping torque. In Fig. 12b, the linear displacements are reversed ($\delta_1 = -1$ mm, $\delta_2 = 1$ mm): the distortion shows a similar pattern with a downward direction imposed by part 1.

5.3 Tolerance stackup

For an example of statistical tolerance analysis, the same materials and part dimensions are assumed as for the example in subsection 5.2. Let $T_{B1} = 2$ mm and $T_{B2} = 1$ mm be the maximum deflections, $T_{F1} = T_{F2} = 0.3$ mm the straightness tolerances, and $\lambda_F = 200$ mm the wavelength of the form error. The analysis will provide the variation T_j on the displacements y_j at the n points along the assembly.

A first solution can be found using the static analogy in the Monte Carlo method. For this purpose, a sample of 100,000 instances of part errors (δ_1, θ_1, δ_2, θ_2) is randomly generated. This is done using the normal distributions with standard deviations in Table 1 for the random error components, and calculating the total errors in the two parts from (12), (13), and (14). The static analogy provides the sensitivity matrix in (6), which allows to calculate the distortions y_j at the points along the assembly using (1). At the end of the simulation, the standard deviations of all y_j are estimated; the resulting variation T_j is plotted in Fig. 13 through its upper and lower 3σ limits. It can be seen that the maximum distortion is close to the joint location on part 2 with a variation of about ±0.6 mm. Although the distortions are possibly asymmetric for individual instances, the variation over the whole sample is relatively symmetric.

Table 3 Distortion of the assembly for the example (static analogy)

Point	x_j, mm	*Description*	$s_{j\delta}$, mm/mm	$s_{j\theta}$, mm/rad	y_j, mm
1	−300	Fixture 1	0	0	0
2	−250	-	0.074	−0.0069	−0.012
3	−200	-	0.259	−0.0222	−0.037
4	−150	-	0.500	−0.0375	−0.058
5	−100	-	0.741	−0.0444	−0.057
6	−50	-	0.926	0.0347	−0.017
7	0	joint	1	0	0.078
8	50	-	0.844	0.0281	0.138
9	100	-	0.500	0.0250	0.103
10	150	-	0.156	0.0094	0.036
11	200	Fixture 2	0	0	0

The static analogy does not actually need to be integrated in a Monte Carlo simulation, as it directly provides the sensitivities of the y_j with respect to errors δ_1, θ_1, δ_2, and θ_2. As described in Section 4.3, these sensitivities can be used directly to compute the RSS stackup of part tolerances using (21). For example, the simulation provides the variation limits $T_j = \pm 0.459$ mm for point $j = 21$ with coordinate $x = -0.1$ m. The same result is obtained by using the jth row of the sensitivity matrix in (6):

$$\begin{bmatrix} s_{j1} & s_{j2} & s_{j3} & s_{j4} \end{bmatrix} = \begin{bmatrix} 0.4893 & -0.0702 & 0.2515 & 0.0257 \end{bmatrix} \quad (37)$$

The sensitivities of the distortion variation at the jth point to the specified tolerances are obtained by replacing (37) in Eqs. (22), (23), (24), and (25). Table 5 shows the calculated sensitivities and the result of the stackup from (21). The value of T_j equals the one found by simulation.

Table 5 also shows the percentage contributions of the individual part tolerances to the distortion at the point; these are given by the corresponding terms in (21) divided by the squared T_j. The distortion appears to be mostly determined by the tolerances on part 1, apparently due to its greater stiffness. Furthermore, form errors give a greater contribution than deflections despite the lower tolerances. This is consistent with the considerations made in Section 5.2: the clamping torque due to the independence between linear and angular form errors causes asymmetrical distortion patterns that seem to have a major impact on the overall deviation from the nominal profile of the assembly.

6 Discussion

The results of Section 5 suggest some considerations about the potential of the static analogy as an alternative to existing methods (DMC and MIC). As said before, the comparison is limited to a particularly simple problem, not representative of the real-world applications where the two methods

Table 4 Displacements at selected points for the example (direct method)

i	*Error*	F_i, N	M_i, Nm	y_{i3}, mm	y_{i7}, mm	y_{i9}, mm
1	δ_1	−0.031	0.0047	0.189	0.498	0.182
2	θ_1	0.035	−0.0070	−0.218	−0.405	−0.075
3	δ_2	−0.013	−0.0013	−0.070	−0.502	−0.318
4	θ_2	−0.012	−0.0016	0.062	0.486	0.315
-	Total	−0.021	−0.0052	−0.037	0.078	0.103

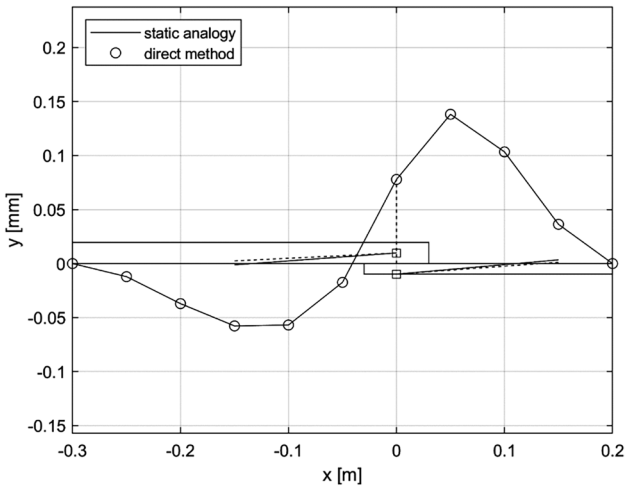

Fig. 11 Distortion of the assembly for the example (comparison)

have been extensively proven in literature with commercial software implementations.

The proposed method allows the direct linearization of the tolerance analysis problem, i.e., the evaluation of the first-order sensitivities of the output error with respect to the input errors. This property is commonly recognized as the main advantage of the MIC over the DMC, which repeats the calculation of output errors a large number (at least thousands) of times to estimate their standard deviations. Like the MIC, therefore, the static analogy allows to calculate the tolerance stackup without the need to wrap the procedure in Monte Carlo simulation. Assuming normal distributions for the random errors, the confidence limits of the distortion at each point can be estimated with an RSS equation, possibly with covariance terms taking into account statistical dependencies between part errors. The reduction in computing time with respect to simulation is negligible in the two-dimensional PCWR case, but could be relevant for more complex cases of compliant tolerance analysis.

Compared to the MIC, the static analogy requires more FEM runs to calculate the sensitivities, but on models with generally fewer elements. For the example of Section 5.2, the first step of both methods involves four runs (one for each input error) on a single-element model. In the second step, the MIC would have required only two runs (forces and torques on the assembly) on a model with 50 elements (n_1+n_2). The static analogy has required 30 runs on a model with 30 elements (n_1) and 20 runs on a model with 20 elements (n_2). With an overhead for the setup of the stiffness matrices, the same calculation could have been done with 50 runs on different models, each with just two elements. The difference in computing times is negligible in this case, but could be noticeable in perspective applications to either 3D problems or bent sheet metal parts. Overall, the disadvantage

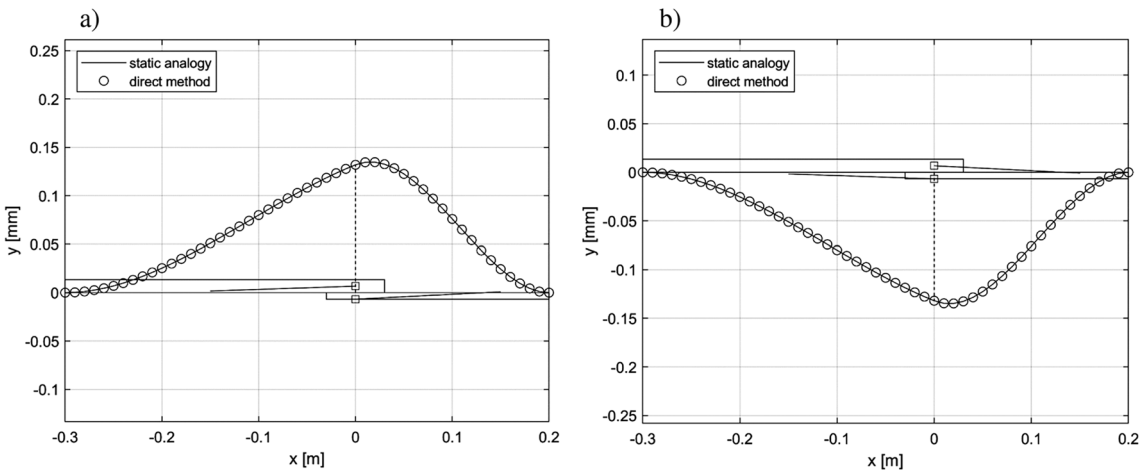

Fig. 12 Cases with pure bending: **a** same δ_i; **b** inverted δ_i

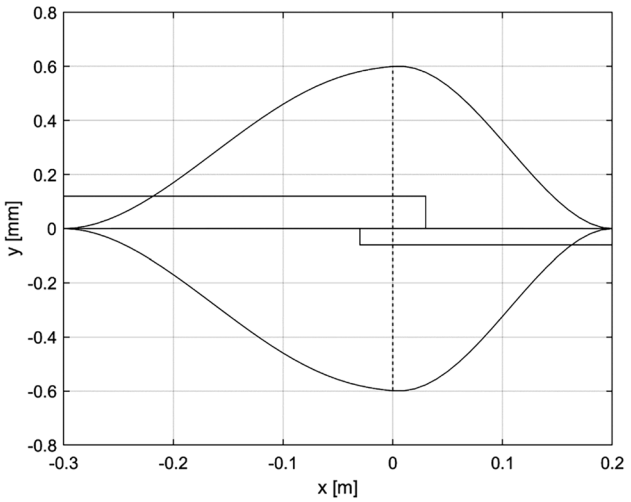

Fig. 13 Confidence intervals of the distortions along the assembly for the example

of the static analogy decreases if the number of input errors increases and if the distortion is to be estimated at fewer points.

The static analogy was initially proposed to solve 2D tolerance analysis problems on rigid parts with hand calculations. This has been shown to be feasible also in simple cases with compliant parts, as in the symmetric PCWR case of Section 5.1. The calculation of the sensitivities of errors δ and θ at the joint location boils down to the resolution of a fixed–fixed beam with uniform section under two symmetrical loading conditions, allowing the straightforward use of known results. In comparison, the same sensitivities are calculated with a long analytical derivation using the direct method, and by solving a larger number of static models (four cantilever beams and eight fixed–fixed beams) using the MIC. The calculation of the sensitivities at the individual points of the assembly would have simply required finding the support reactions of a doubly fixed beam with unsymmetrical load, also available in statics textbooks. In all cases, the static analogy requires a simpler procedure than the other methods, because it does not require any calculation of deflections from external forces or vice versa.

7 Conclusions

The paper has proposed a new method for compliant tolerance analysis, which extends the static analogy already proposed for the corresponding problem with rigid parts. The method has been applied to the PCWR case on flat rectangular parts, treated as a 2D problem with straight beam elements. Although such case is only the simplest of the possible applications of the problem, it has allowed to verify the correctness and the potential of the method. The results confirm that it gives correct results in comparison with existing methods through both analytical derivation and FEM analysis. They also show that it has a different workflow from other methods, and that it can be easily applied to problems of statistical tolerance analysis.

Table 5 Tolerance stackup at point $j=21$ for the example

Tolerance	*Value*, mm	*Sensitivity*	*Contribution*, %
T_{B1}	2	0.1383	36
T_{F1}	0.3	1.1295	54
T_{B2}	1	0.0587	2
T_{F2}	0.3	0.4228	8
$\rightarrow T_j$	0.459	-	(100)

The proposed method allows the calculation of the first-order sensitivities of the output errors on the assembly to the input errors on the individual parts. Under the assumptions of small displacements and normal distributions of errors, the linearization avoids the use of Monte Carlo simulation. This is an advantage on the DMC approach, which involves a high computational effort due to the need to repeat the FEM analysis for many random instances of part errors. On the other hand, the static analogy cannot easily be extended to nonlinear problems involving material plasticity or thermomechanical effects of welding, where DMC has been tested through more advanced formulations.

Compared to the MIC, the linearization requires a higher number of FEM runs but on lighter models, with a predictable disadvantage in overall efficiency. However, the static analogy does not require the calculation of deflections, but finds the sensitivities through the sole calculation of support reactions and internal forces. For the simple cases dealt with in the paper, this implies that the distortion of the assembly can also be calculated using known results of statics, avoiding the use of FEM analysis. Without further evidence, it is obviously not said that such advantage can be possibly achieved when scaling the method to more complex problems.

Another contribution of the work is a procedure for the random generation of part errors. Each of them is decomposed into a form error and a deflection, so that the covariances between linear and angular errors could be easily included in the RSS stackup equation. The application example has shown that the two error components have qualitatively different effects on the distortion profile due to possible clamping torques.

The above results seem to encourage the further development of the static analogy, with the aim of dealing with PCWR cases on bent sheet metal parts and generic 3D problems of compliant tolerance analysis. Such goal will require

more complex FEM modeling as well as the solution of problems already addressed in the MIC, such as geometric covariance and contact modeling. At the same time, it will be investigated whether approximate force analysis on 3D overconstrained parts can provide a possible alternative to FEM in supporting streamlined manual or computer-based calculations.

Authors contribution Not applicable.

Funding Open access funding provided by Politecnico di Milano within the CRUI-CARE Agreement.

Data availability The author confirms that the data supporting the findings of this study are available within the paper.

Code availability Not applicable.

Declarations

Conflict of interest The authors declare no competing interests.

References

1. Singh PK, Jain PK, Jain SC (2009) Important issues in tolerance design of mechanical assemblies. Part I: tolerance analysis. Proc IMechE B J Eng Manuf 223:1225–1247
2. Cao Y, Liu T, Yang J (2018) A comprehensive review of tolerance analysis models. Int J Adv Manuf Technol 97:3055–3085
3. Liu SC, Hu SJ (1997) Variation simulation for deformable sheet metal assemblies using finite element methods. Trans ASME J Manuf Sci Eng 119:368–374
4. Liu SC, Hu SJ (1995) An offset finite element model and its applications in predicting sheet metal assembly variation. Int J Mach Tool Manuf 35(11):1545–1557
5. Shiu BW, Ceglarek D, Shi J (1997) Flexible beam-based modeling of sheet metal assembly for dimensional control. Trans NAMRI/SME 25:49–54
6. Ceglarek DJ, Shi J (1997) Tolerance analysis for sheet metal assembly using a beam-based model. Proc ASME IMECE 15:153–160
7. Liu SC, Hu SJ, Woo TC (1996) Tolerance analysis for sheet metal assemblies. Trans ASME J Mech Des 118:62–67
8. Liu SC, Hu SJ (1997) A parametric study of joint performance in sheet metal assembly. Int J Mach Tool Manuf 37(6):873–884
9. Hu M, Lin Z, Lai X, Ni J (2001) Simulation and analysis of assembly processes considering compliant, non-ideal parts and tooling variations. Int J Mach Tool Manuf 41:2233–2243
10. Camelio J, Hu SJ, Ceglarek D (2003) Modeling variation propagation of multi-station assembly systems with compliant parts. ASME J Mech Des 125:673–681
11. Hu SJ (1997) Stream-of-variation theory for automotive body assembly. CIRP Ann 46(1):1–6
12. Jin J, Shi J (1999) State space modeling of sheet metal assembly for dimensional control. Trans ASME J Manuf Sci Eng 121:756–762
13. Camelio JA, Hu SJ, Marin SP (2004) Compliant assembly variation analysis using component geometric covariance. ASME J Manuf Sci Eng 126:355–360
14. Liu YG, Hu SJ (2005) Assembly fixture fault diagnosis using designated component analysis. Trans ASME J Manuf Sci Eng 127:358–368
15. Camelio JA, Hu SJ (2004) Multiple fault diagnosis for sheet metal fixtures using designated component analysis. ASME J Manuf Sci Eng 126:91–97
16. Liao X, Wang GG (2005) Employing fractals and FEM for detailed variation analysis of non-rigid assemblies. Int J Mach Tool Manuf 45:445–454
17. Matuszyk TI, Cardew-Hall MJ, Rolfe BF (2010) The kernel density estimate/point distribution model (KDE-PDM) for statistical shape modeling of automotive stampings and assemblies. Robot Comput Integr Manuf 26:370–380
18. Lindau B, Lindkvist L, Andersson A, Söderberg R (2013) Statistical shape modeling in virtual assembly using PCA-technique. J Manuf Syst 32:456–463
19. Zheng H, Litwa F, Reese B, Li C, Bohn M, Paetzold K (2019) A modeling approach for elastic tolerance simulation of the body in white hang-on parts. Proc ICED 3461–3470
20. Dahlström S, Lindkvist L (2007) Variation simulation of sheet metal assemblies using the method of influence coefficients with contact modeling. ASME J Manuf Sci Eng 129:615–622
21. Wärmefjord K, Lindkvist L, Söderberg R (2008) Tolerance simulation of compliant sheet metal assemblies using automatic node-based contact detection. Proc ASME IMECE 66344
22. Ungemach G, Mantwill F (2009) Efficient consideration of contact in compliant assembly variation analysis. ASME J Manuf Sci Eng 131:011005
23. Lindau B, Lorin S, Lindkvist L, Söderberg R (2016) Efficient contact modeling in nonrigid variation simulation. ASME J Comput Inf Sci Eng 16:011002
24. Lorin S, Lindkvist L, Söderberg R (2016) Variation simulation of stresses using the method of influence coefficients. ASME J Comput Inf Sci Eng 14:011001
25. Söderberg R, Wärmefjord K, Lindkvist L (2015) Variation simulation of stress during assembly of composite parts. CIRP Annals Manuf Technol 64:17–20
26. Sellem E, Rivière A (1998) Tolerance analysis of deformable assemblies. Proc ASME DETC/DAC-5571
27. Sellem E, Rivière A, De Hillerin CA, Clement A (1999) Validation of the tolerance analysis of compliant assemblies. Proc ASME DETC/DAC-8678
28. Gerbino S, Patalano S, Franciosa P (2008) Statistical variation analysis of multi-station compliant assemblies based on sensitivity matrix. Int J Comput Appl Technol 33(1):12–23
29. Franciosa P (2009) Modeling and simulation of variational rigid and compliant assembly for tolerance analysis. PhD thesis, University of Naples Federico II
30. Franciosa P, Gerbino S, Patalano S (2013) A computer-aided tool to quickly analyse variabilities in flexible assemblies in different design scenarios. Int J Prod Dev 18(2):112–133

31. Corrado A, Polini W, Giuliano G (2019) Super-element method applied to MIC to reduce simulation time of compliant assemblies. Int J Comput Appl Technol 59:277
32. Corrado A, Polini W (2019) A new way to solve tolerance analysis: The Cassino unified tolerance analysis tool. Int J Comput Integr Manuf 32(2):124–135
33. Polini W, Corrado A (2020) Methods of influence coefficients to evaluate stress and deviation distribution of flexible assemblies: A review. Int J Adv Manuf Technol 107:2901–2915
34. Lee B, Shalaby MM, Collins RJ, Crisan V, Walls SA, Robinson DM, Saitou K (2007) Variation analysis of three dimensional nonrigid assemblies. Proc Int Symp Assem Manuf, MoA1.3
35. Cai N, Qiao L, Anwer N (2015) Unified variation modeling of sheet metal assembly considering rigid and compliant variations. Proc IMechE Part B J Eng Manuf 229(3):495–507
36. Yu K, Jin S, Lai X, Xing Y (2008) Modeling and analysis of compliant sheet metal assembly variation. Assem Autom 28(3):225–234
37. Yu KG, Yang ZH (2015) Assembly variation modeling method research of compliant automobile body sheet metal parts using the finite element method. Int J Autom Technol 16(1):51–56
38. Lindau B, Wärmefjord K, Lindkvist L, Söderberg R (2014) Method for handling model growth in nonrigid variation simulation of sheet metal assemblies. ASME J Comput Inf Sci Eng 14:031004
39. Merkley KG (1998) Tolerance analysis of compliant assemblies. PhD thesis, Brigham Young University
40. Bihlmaier BF (1999) Tolerance analysis of flexible assemblies using finite element and spectral analysis. ADCATS Rep 99–1, Brigham Young University
41. Mortensen AJ (2002) An integrated methodology for statistical tolerance analysis of flexible assemblies. MS thesis, Brigham Young University
42. Stewart ML (2004) Variation simulation of fixtured assembly processes for compliant structures using piecewise-linear analysis. MS thesis, Brigham Young University
43. Liao X, Wang GG (2007) Non-linear dimensional variation analysis for sheet metal assemblies by contact modeling. Finite Element Analysis Des 44:34–44
44. Lupuleac S, Kovtun M, Rodionova O, Marguet B (2009) Assembly simulation of riveting process. SAE Int J Aerosp 2(1):193–198
45. Xie K, Wells L, Camelio JA, Youn BD (2007) Variation propagation analysis on compliant assemblies considering contact interaction. Trans ASME J Manuf Sci Eng 129:934–942
46. Hashemian A, Imani BM (2014) An improved sensitivity-free probability analysis in variation assessment of sheet metal assemblies. J Eng Des 25(10–12):346–366
47. Hashemian A, Imani BM (2014) Surface fairness: A quality metric for aesthetic assessment of compliant automotive bodies. J Eng Des 29(1):41–64
48. Liu T, Li ZM, Jin S, Chen W (2019) Compliant assembly analysis including initial deviations and geometric nonlinearity. Part I: Beam structure. Proc IMechE Part C J Mech Eng Sci 233(12):4233–4246
49. Liu T, Li ZM, Jin S, Chen W (2019) Compliant assembly analysis including initial deviations and geometric nonlinearity. Part II: plate structure. Proc IMechE Part C J Mech Eng Sci 233(11):3717–3732
50. Liu C, Liu T, Du J, Zhang Y, Lai X, Shi J (2020) Hybrid nonlinear variation modeling of compliant metal plate assemblies considering welding shrinkage and angular distortion. ASME J Manuf Sci Eng 142:041003
51. Chang M, Gossard DC (1997) Modeling the assembly of compliant, non-ideal parts. Comput Aided Des 29–10:701–708
52. Ni J, Tang W, Xing Y (2014) Three-dimensional precision analysis with rigid and compliant motions for sheet metal assembly. Int J Adv Manuf Technol 73:805–819
53. Schlather F, Oefele F, Zaeh MF (2016) Toward a feature-based approach for fixtureless build-up of sheet metal structures. Int J Eng Tech Res 5(4):2454–4698
54. Schlather F, Hoesl V, Oefele F, Zaeh MF (2018) Tolerance analysis of compliant, feature-based sheet metal structures for fixtureless assembly. J Manuf Sys 49:25–35
55. Franciosa P, Gerbino S, Patalano S (2011) Simulation of variational compliant assemblies with shape errors based on morphing mesh approach. Int J Adv Manuf Technol 53:47–61
56. Mazur M, Leary M, Subic A (2015) Application of polynomial chaos expansion to tolerance analysis and synthesis in compliant assemblies subject to loading. ASME J Mech Des 137:031701
57. Aghabeigi M, Khodaygan S, Movahhedy MR (2022) Tolerance analysis of a compliant assembly using random Non-Uniform Rational B-Spline curves and isogeometric method. J Comput Des Eng 9:2170–2195
58. Hughes TJR, Cottrell JA, Bazilevs Y (2005) Isogeometric analysis: CAD, finite elements, NURBS, exact geometry and mesh refinement. Comput Method Appl Mech Eng 194:4135–4195
59. Wärmefjord K, Söderberg R, Lindkvist L (2010) Variation simulation of spot welding sequence for sheet metal assemblies. Proc NordDesign 519–528
60. Liu G, Huan H, Ke Y (2014) Study on analysis and prediction of riveting assembly variation of aircraft fuselage part. Int J Adv Manuf Technol 75:881–1003
61. Pahkamaa A, Wärmefjord K, Karlsson L, Söderberg R, Goldak J (2014) Combining variation simulation with welding simulation for prediction of deformation and variation of a final assembly. ASME J Comput Inf Sci Eng 12:021002
62. Lorin S, Cromvik C, Edelvik F, Lindkvist L, Söderberg R (2014) Variation simulation of welded assemblies using a thermo-elastic finite element model. ASME J Comput Inf Sci Eng 14:031003
63. Choi W, Chung H (2015) Variation simulation of compliant metal plate assemblies considering welding distortion. ASME J Manuf Sci Eng 137:031008
64. Zhang T, Shi J (2016) Stream of variation modeling and analysis for compliant composite part assembly. Part I: Single-station processes. ASME J Manuf Sci Eng 138:121003
65. Jareteg C, Wärmefjord K, Cromvik C, Söderberg R, Lindkvist L, Carlson J, Larsson S, Edelvik F (2016) Geometry assurance integrating process variation with simulation of spring-in for composite parts and assemblies. ASME J Comput Inf Sci Eng 16:031003
66. Apley DW, Shi J (1998) Diagnosis of multiple fixture faults in part assembly. Trans ASME J Manuf Sci Eng 120:793–801
67. Rong Q, Ceglarek D, Shi J (2000) Dimensional fault diagnosis for compliant beam structure assemblies. ASME J Manuf Sci Eng 122:773–780
68. Camelio JA, Hu SJ, Ceglarek D (2004) Impact of fixture design on sheet metal assembly variation. J Manuf Syst 23(3):182–193
69. Ceglarek D, Prakash PKS (2012) Enhanced piecewise least squares approach for diagnosis of ill-conditioned multistation assembly with compliant parts. Proc IMechE Part B J Eng Manuf 226:485–502
70. Li B, Shiu BW, Lau KJ (2001) Principle and simulation of fixture configuration design for sheet metal assembly with laser welding. Part 1: Finite-element modelling and a prediction and correction method. Int J Adv Manuf Technol 18:266–275
71. Söderberg R, Lindkvist L, Dahlström S (2006) Computer-aided robustness analysis for compliant assemblies. J Eng Des 17(5):411–428
72. Shiu BW, Apley DW, Ceglarek D, Shi J (2003) Tolerance allocation for compliant beam structure assemblies. IIE Trans 35(4):329–342
73. Li Z, Yue J, Kokkolaras M, Camelio J, Papalambros PY, Hu SJ (2004) Product tolerance allocation in compliant multistation

assembly through variation propagation and analytical target cascading. Proc ASME IMECE 60521
74. Zheng H, Litwa F, Bohn M, Paetzold K (2021) Tolerance optimization for sheet metal parts based on joining simulation. Procedia CIRP 100:583–588
75. Wärmefjord K, Carlson JS, Söderberg R (2016) Controlling geometrical variation caused by assembly fixtures. ASME J Comput Inf Sci Eng 16:011007
76. Tabar RS, Wärmefjord K, Söderberg R (2019) A method for identification and sequence optimisation of geometry spot welds in a digital twin context. Proc IMechE Part C J Mech Eng Sci 233(16):5610–5621
77. Tabar RS, Wärmefjord K, Söderberg R, Lindkvist L (2020) Efficient spot welding sequence optimization in a geometry assurance digital twin. ASME J Mech Des 142:102001
78. Tabar RS, Lorin S, Cromvik C, Lindkvist L, Wärmefjord K, Söderberg R (2021) Efficient spot welding sequence optimization in a compliant variation simulation. ASME J Manuf Sci Eng 143:071009
79. Söderberg R, Lindkvist L, Wärmefjord K, Carlson JS (2016) Virtual geometry assurance process and toolbox. Procedia CIRP 43:3–12
80. Söderberg R, Wärmefjord K, Carlson JS, Lindkvist L (2017) Toward a digital twin for real-time geometry assurance in individualized production. CIRP Annals Manuf Technol 66(2017):137–140
81. Armillotta A (2014) A static analogy for 2D tolerance analysis. Assem Autom 34(2):182–191
82. Armillotta A (2015) Force analysis as a support to computer-aided tolerancing of planar linkages. Mech Mach Theory 93:11–25
83. Armillotta A (2019) Tolerance analysis of gear trains by static analogy. Mech Mach Theory 135:65–80